Journal of Experimental Botany, Vol. 70, No. 15 pp. 3927–3940, 2019
doi:10.1093/jxb/erz204 Advance Access Publication 30 April, 2019
This paper is available online free of all access charges (see https://academic.oup.com/jxb/pages/openaccess for further details)

RESEARCH PAPER

Systemic signalling through translationally controlled tumour protein controls lateral root formation in Arabidopsis

Rémi Branco and Josette Masle*,

The Australian National University, College of Science, Research School of Biology, Canberra ACT 0200, Australia

* Correspondence: Josette.masle@anu.edu.au

Received 22 January 2019; Editorial decision 15 April 2019; Accepted 6 April 2019

Editor: James Murray, Cardiff University, UK

Abstract

The plant body plan and primary organs are established during embryogenesis. However, in contrast to animals, plants have the ability to generate new organs throughout their whole life. These give them an extraordinary developmental plasticity to modulate their size and architecture according to environmental constraints and opportunities. How this plasticity is regulated at the whole-organism level is elusive. Here we provide evidence for a role for translationally controlled tumour protein (TCTP) in regulating the iterative formation of lateral roots in Arabidopsis. AtTCTP1 modulates root system architecture through a dual function: as a general constitutive growth promoter enhancing root elongation and as a systemic signalling agent via mobility in the vasculature. *AtTCTP1* encodes mRNAs with long-distance mobility between the shoot and roots. Mobile shoot-derived *TCTP1* gene products act specifically to enhance the frequency of lateral root initiation and emergence sites along the primary root pericycle, while root elongation is controlled by local constitutive TCTP1 expression and scion size. These findings uncover a novel type for an integrative signal in the control of lateral root initiation and the compromise for roots between branching more profusely or elongating further. They also provide the first evidence in plants of an extracellular function of the vital, highly expressed ubiquitous TCTP1.

Keywords: Grafts, lateral root initiation, long-distance mobility, TCTP, translationally controlled tumour protein, root development, root system architecture, scion control of rootstock development.

Introduction

Plant development is highly plastic. This is essential to survival and adaptation to a wide range of environments from which, being sessile, plants cannot escape. That plasticity manifests itself as an extraordinary capacity of the plant to modify the number, size, shape, patterning, and spatial deployment of its organs, above and below ground, to adapt efficiently to environmental constraints.

As is typical of dicotyledonous species, the Arabidopsis root system arises from a primary root, initiated in the embryo, and *de novo* organogenesis of secondary and higher order lateral roots (LRs), post-embryonically (Peret et al., 2009; Bellini *et al.*, 2014). LRs constitute the major part of the root system, and are major determinants of water and nutrient uptake and colonization of new soil pockets. Despite their high agronomic and ecological relevance, the molecular mechanisms that determine the placement of LRs, in space and time, and their number are still little known. LRs originate from inner root pericycle founder cells, through a pre-patterning (priming) activation and cell fate re-definition process that gives them competence to divide and differentiate in an orderly fashion to generate a highly organized root primordium (Malamy and Benfey, 1997; De Smet *et al.*, 2007; Peret *et al.*, 2009; Moreno-Risueno *et al.*, 2010). The

establishment of LR initiation sites and the subsequent actual initiation process are not well understood. They are thought to involve an oscillating transcriptional network in interaction with auxin and other as yet unidentified mobile signals and to depend critically on intercellular connectivity (De Smet *et al.*, 2007; Moreno-Risueno *et al.*, 2010; Benitez-Alfonso *et al.*, 2013).

There is intense trafficking of a vast array of molecules between shoot and roots—photoassimilates and a range of growth-enabling metabolites, numerous hormones, and also a vast number of proteins and RNAs (Turgeon and Wolf, 2009; Batailler *et al.*, 2012; Turnbull and Lopez-Cobollo, 2013; Kim *et al.*, 2014; Thieme *et al.*, 2015). Besides specialized miRNAs and siRNAs, translocated RNAs include a huge cohort of protein-encoding mRNAs of various kinds. It is now well recognized that hundreds to thousands of mRNAs transit in the phloem and have long-distance mobility between aerial organs and roots (Notaguchi *et al.*, 2015; Thieme *et al.*, 2015; Yang *et al.*, 2015; W. Zhang *et al.*, 2016; Xia *et al.*, 2018). Long-distance movement of proteins has also been demonstrated, many of which can be unloaded in the root tip (Atkins *et al.*, 2011; Paultre *et al.*, 2016). An emerging consensus is that this movement does not simply reflect passive diffusion and mass flow, but is in part an actively controlled movement, probably serving for the delivery of systemic signalling agents (Jorgensen *et al.*, 1998; Lough and Lucas, 2006; Calderwood *et al.*, 2016; Paultre *et al.*, 2016; Kehr and Kragler, 2018; Morris, 2018). There are a few established cases of genes regulating plant development through mobility of their mRNA and/or encoded protein, such as FT in the regulation of flowering time (Corbesier *et al.*, 2007; Jaeger and Wigge, 2007), GIBBERELLIC ACID-INSENSITIVE (GAI) or Mouse eras (me) in the regulation of leaf development (Kim *et al.*, 2001; Haywood *et al.*, 2005), the *StBEL5* transcription factor gene in the control of tuber formation (Banerjee *et al.*, 2009), or shoot-derived *Auxin/Indole-3-Acetic Acid IAA18* and *IAA28* in the regulation of LR formation (Notaguchi *et al.*, 2012). However, nothing is known of the physiological significance of the vast majority of mobile mRNAs or proteins transiting through the phloem and roles in receiving cells, nor of the mechanisms controlling their excretion, transport, and delivery.

Among the large number of mRNAs with demonstrated long-distance mobility between above- and below-ground organs are transcripts encoding transcriptionally controlled tumour proteins (TCTPs). These include Arabidopsis *AtTCTP1* (Notaguchi *et al.*, 2015; Thieme *et al.*, 2015) and *AtTCTP2* (Toscano-Morales *et al.*, 2014), a *Vitis vinifera* TCTP (*GSVIVG01017723001*; Yang *et al.*, 2015), or *Csa3M154390*, a *Cucumis* TCTP (Z. Zhang *et al.*, 2016). TCTP is a highly conserved ubiquitous protein found in almost all eukaryotes. Its molecular function is still a matter of debate, but clearly relates to the regulation of GTPase activity (Hsu *et al.*, 2007; Dong *et al.*, 2009). Fitting with this, TCTP is involved in a number of fundamental biological processes. It is known as an essential mitotic factor and a promoter of cellular growth interacting with the protein synthesis machinery, and also as a cytoprotective and anti-apopoptic protein (reviewed by Bommer and Thiele, 2004; Bommer, 2017). Although best characterized in animals given their high relevance to malignancy and cancer progression, these core functions appear largely conserved in other eukaryotes, including plants, and make TCTPs essential proteins for embryogenesis and early development, organ patterning, regulation of organ size, and cellular homeostasis (Bommer, 2017). In Arabidopsis, knock-out mutations of either *AtTCTP1* or its homologue, *AtTCTP2*, are lethal (Berkowitz *et al.*, 2008; Brioudes *et al.*, 2010), as is the case of TCTP loss of function in mice (Chen *et al.*, 2007) or *Drosophila* (Hsu *et al.*, 2007). Reduced *AtTCTP1* expression through RNAi causes general cell proliferation and growth inhibition, in both vegetative and reproductive organs (Berkowitz *et al.*, 2008; Brioudes *et al.*, 2010; Betsch *et al.*, 2019), and plant TCTPs have been linked to resistance to various abiotic stresses, including salinity, drought, flooding, and suboptimal temperatures (Cao *et al.*, 2010; Kim *et al.*, 2012; Li *et al.*, 2013; Chen *et al.*, 2014; Deng *et al.*, 2016; de Carvalho *et al.*, 2017), and also to biotic stresses (Malter and Wolf, 2011; Du *et al.*, 2015; Gawehns *et al.*, 2015).

In addition to its core functions at the cellular level, mammalian TCTP has long been known to act as an extracellular protein in the immune system, and was in fact first characterized as a histamine-releasing factor (HRF) (MacDonald *et al.*, 1995). Human TCTP has since been shown to modulate the release of cytokines and other signalling molecules (MacDonald, 2012) and to have a broad role in immunity (reviewed in MacDonald, 2017). Whether plant TCTPs also assume non-cell-autonomous functions is unknown. The demonstrated long-distance translocation of TCTP transcripts and proteins between scion and rootstock in various species would support that possibility, but in itself does not prove it. Another most interesting indication in that direction is the earlier finding by Aoki et al. (2005) that pumpkin TCTP (CmaCh11G012000) moved rootward in a selectively destination-controlled manner when introduced in rice sieve tubes, and furthermore in complex with RNA-binding proteins and the conserved eukaryotic translation initiation factor eIF5A. Moreover, this association was found to be necessary for the selective movement of the protein complex.

Together, these observations raise the prospect that plant TCTPs might have physiologically important systemic signalling functions, through mobility. This is what we sought to examine, focusing on Arabidopsis *AtTCTP1* (Berkowitz *et al.*, 2008). We asked whether long-distance movement of *AtTCTP1* gene products occurs under physiological conditions and plays a role in shaping root architecture.

Materials and methods

Plant material and growth conditions

The transgenic *proTCTP1::gTCTP1-GFP::NOS* (*TCTP1-GFP*) and the *TCTP1-RNAi* lines are as in Berkowitz *et al.* (2008), and the *35S::YFP-cDNATCTP1* is as in Thieme *et al.* (2015). All lines are in the *Arabidopsis thaliana* Columbia (Col-0) background (wild type, WT).

The hypocotyl micro-grafting method is as in Marsch-Martínez *et al.* (2013) with minor adaptations. Seeds were surface-sterilized for 5 min with a solution of sodium 0.125% (v/v) hypochlorite and 90% (v/v) ethanol, rinsed in 100% ethanol, and dried before being resuspended in sterile water and sown on the surface of a nitrocellulose membrane strip (membrane filter; cellulose nitrate 0.45 μm diameter, Whatman code NC45ST) laid on top of a nutrient agar gel [2.15 g l^{-1} Murashige and Skoog (MS) salts, 0.5% sucrose, 1% agar type-M, pH 5.7] in Petri plates.

The plates were sealed with porous micropore tape (3M), stratified for 2 d at 4 °C in the dark, and incubated in a vertical position at 21 °C, under a 12 h photoperiod with 120 µmol quanta m^{-2} s^{-1} light intensity. Four to six days later, under sterile conditions, the two cotyledons were severed and the seedlings positioned with the hypocotyl perpendicular to the nitrocellulose strip, and the shoot (scion) overhanging on the agar. A sharp cut was then made through the hypocotyl. The upper part (scion) and bottom part (rootstock) were grafted onto the relevant rootstock and scion, respectively, as indicated, by simple hydrophilic contact maintained by dint of water surface tension, ensuring cotyledon petioles were slightly above the agar surface. This generated reciprocal heterografts (WT scion/transgenic rootstock and transgenic scion/WT rootstock) and homografts (scion and rootstock of the same genotype). The plates were resealed and returned to the growth chamber. Five days later (5 DAG, 5 days after grafting), the seedlings were transferred to larger plates filled with similar medium but without sucrose. For the auxin experiment, 20 µM NPA (*N*-1-naphthylphthalamidic acid in DMSO) or an appropriate volume of DSMO solvent was supplied to the medium, and the thickness of agar gel underneath the scion was removed to prevent any contact with the scion. All scion–rootstock combinations compared within an experiment were raised alongside each other within each replicated plate.

For soil-grown plants, on 5 DAG, grafted seedlings were transferred to pots filled with seed raising mix and Osmocote (5g l^{-1}), and then raised alongside seedlings in plates, in the same growth chamber.

Microscopy

For *in vivo* confocal microscopy, the root, scion, or part thereof were mounted on slides in half-strength MS (0% sucrose, pH 5.7, 21 °C) and imaged using a TCS-SP8 microscope (Leica, Germany) equipped with a ×10/0.3 NA or ×63/1.2 NA water immersion objective. Autofluorescence spectra were acquired on the same samples for spectral unmixing. Autofluorescence was excited using a 488 nm argon laser and acquired in λ-mode (from 495 nm to 600 nm, 5 nm acquisition window) with the pinhole opened at 2.8 Airy units (AU). The same parameters were used to acquire green fluorescent protein (GFP) or yellow fluorescent protein (YFP) fluorescence, and spectra were subsequently unmixed using LAS-X (Leica) software. For monitoring the patterns of appearance of scion-derived TCTP1–GFP fluorescence in the root, the whole primary root was imaged daily from 2 DAG, when graft junctions were strong enough, in *x*,*y*-mode. The fluorescence was acquired with a ×10/0.3 NA objective and a 510–525 nm acquisition window, keeping all settings constant within an experiment, and each positive signal was confirmed by spectral unmixing.

For light microscopy, samples were mounted in water, and imaged in DIC (differential interferential contrast) mode with a Leica DM5000B microscope fitted with a ×40/0.85 NA dry objective and a Leica DFC 310FX camera Leica Instruments). Individual cell lengths were measured along epidermal files from the quiescent centre to the root differentiation zone, using a custom macro in Fiji (code available upon request). Mature cell length was estimated by means of 10 consecutive cells in the root differentiation zone.

Phenotyping

For determination of the kinetics of root elongation, plates were scanned daily from seed germination at a resolution of 600 dpi, 8-bits per channel, and saved in Jpeg. The raw images were automatically pre-processed with a custom 'auto align' macro in Fiji, and root lengths (l) were measured using RootTrace as described in French *et al.* (2009). At least six plants per condition with a complete trace were available for each of the compared genotypes and conditions, and thus were used for subsequent analysis. Traces of the primary root were manually curated, and erroneous data were manually corrected using the 'segmented line' tool in Fiji software. The relative root elongation rate (RER; mm mm^{-1} h^{-1}) was computed for each root as:

$$RER(t) = dl/dt \times l/t$$

For normalization of average scion size between WT/RNAi and RNAi/WT grafts, at 12 DAG (i.e. a week after the grafted seedlings had been transferred to a new plate as described above), the first leaf of WT scions was severed from half of the WT/RNAi heterografts, generating WT_{AMP} scions, and left intact in the other half. To minimize potential artefacts due to confounding wounding effects when comparing amputated WT_{AMP} scions and scions left intact (WT or RNAi), one of the cotyledon stumps in these grafts was gently squeezed with a pair of very fine tweezers. All plates were scanned daily. Primary and secondary LR lengths were determined using Fiji software.

Scion sizes were measured in all grafts at the end of each experiment through destructive sampling, laying leaves flat on a film of 0.8% phytagel without overlaps, and scanning them at 2400 dpi resolution for leaf area measurement using Fiji. Roots were fixed in a fixing solution [phosphate-buffered saline, 10% (v/v) formaldehyde, 0.1% (v/v) Triton X-100], and imaged by light microscopy in DIC mode. Epidermal cell length profiles along the primary root were determined using the macro 'Cell length profile'. The positions of all non-emerged lateral root primordia (LRPs) and emerged LRs between the root–hypocotyl junction and root tip were recorded. The distance between the most basal (oldest) LR and the most acropetal LRP was defined as the 'zone of lateral root formation and emergence', enabling determination of LRP and LR densities along that zone (number mm^{-1}).

Molecular analysis

For quantitative reverse transcription PCR (qRT–PCR), fresh tissues were snap-frozen in liquid nitrogen and ground using a Tissue Lyzer (Quiagen). Total RNA was obtained using a chloroform/TRIzol (Thermofisher) extraction protocol, following the manufacturer's instructions. mRNAs were purified from 40 µg of total RNA using TYGR Dynabeads® oligo$(dT)_{25}$ and subsequently used for cDNA synthesis using 200 U of M-MLV (Promega). The qRT–PCR was performed with 2.5 µl of the diluted reverse transcriptase mix in a final volume of 10 µl of FastStart Universal SYBR® Green Master (Roche) and using a VIIA7 real-time PCR system (Thermofisher). Primer efficiencies were calculated using LinRegPCR (Ramakers *et al.*, 2003), and the relative expression of target genes was normalized to four reference genes (*TIP41*, *APT1*, *UBC9*, and *PDF2*) using the delta-Ct method (Livak and Schmittgen, 2001). Primers used for quantification of *AtTCTP1* and reference gene mRNAs are as in Berkowitz *et al.* (2008). GFP-specific primers were either $GFP1_{for}$ 5'GATCCTGTTGACGAGGGTGT3' and $GFP1_{rev}$ 5'GGATACGTGCAGGAGAGGAC3', or $GFP2_{for}$ 5'GATGCCGTTCTTTTGCTTGTCG3' and $GFP2_{rev}$ 5'CGTGC AGTGCTTCTCCCGTTAC3'. The two sets of primers produced almost identical delta-Ct values, which were thus averaged to calculate expression levels. Primers for quantification of *CycB1;1* expression were $CycB1;1_{for}$ 5'TCAGCTCATGGACTGTGCAA3' and $CycB1;1_{rev}$ 5'GATCAAAGCCACAGCGAAGC3'. In all experiments, measurements were replicated on 3–6 independent pools, each consisting of scion or rootstocks from at least five plants, unless specified otherwise.

Statistical analysis

Data were analysed and plotted using the OriginPro software v9. This includes curve fittings, tests for equal variance (Levene), and ANOVA followed by post-hoc tests for pair-wise comparisons (Tukey or Bonferroni, as appropriate).

Gene accessions numbers

AtAPT1 (*At1g27450*), *AtCyclinB-1* (*At4g37490*), *AtPDF2* (*At1g13320*), *AtTCTP1* (*At3g16640*), *AtTCTP2* (*At3g05540*), *AtTIP41* (*At4g34270*), *AtUBC9* (*At4g27960*).

Results

AtTCTP1 *mRNA moves through the shoot–root graft junction, in both directions*

To investigate the long-distance mobility of endogenous *AtTCTP1* mRNA and its encoded protein in a physiologically

relevant context, and to be able to differentiate between locally expressed *AtTCTP1* and *AtTCTP1* originating from distant sources, we performed reciprocal grafts between WT (Col-0) and a TCTP1–GFP line expressing a AtTCTP1–GFP fusion protein under the control of the *AtTCTP1* native promoter (*pAtTCTP1::gAtTCTP1-GFP* (Berkowitz *et al.*, 2008; Fig. 1A). To avoid potential confounding effects from the uncontrolled formation of adventitious roots post-grafting, we developed a modified micro-grafting technique where these roots are not formed (see the Materials and methods). At 14 DAG, the scions had developed 5–6 leaves of normal size (Fig. 1B), indicating that the scion–rootstock junction was fully functional. Microscopic observation confirmed a clean junction, with continuous vasculature and absence of adventitious root primordia (Fig. 1C–F).

TCTP1-GFP transcripts were detected in both the scion of WT/TCTP1–GFP grafts and the rootstock of TCTP1–GFP/WT reciprocal grafts. This was observed in young seedlings grown *in vitro* (14 DAG; Fig. 1G) and also at a much later stage (early flowering) in soil-grown grafts (80 DAG; Fig. 1H). Mobile *TCTP1-GFP* transcripts were more abundant in the latter, both in absolute terms and relative to the amount

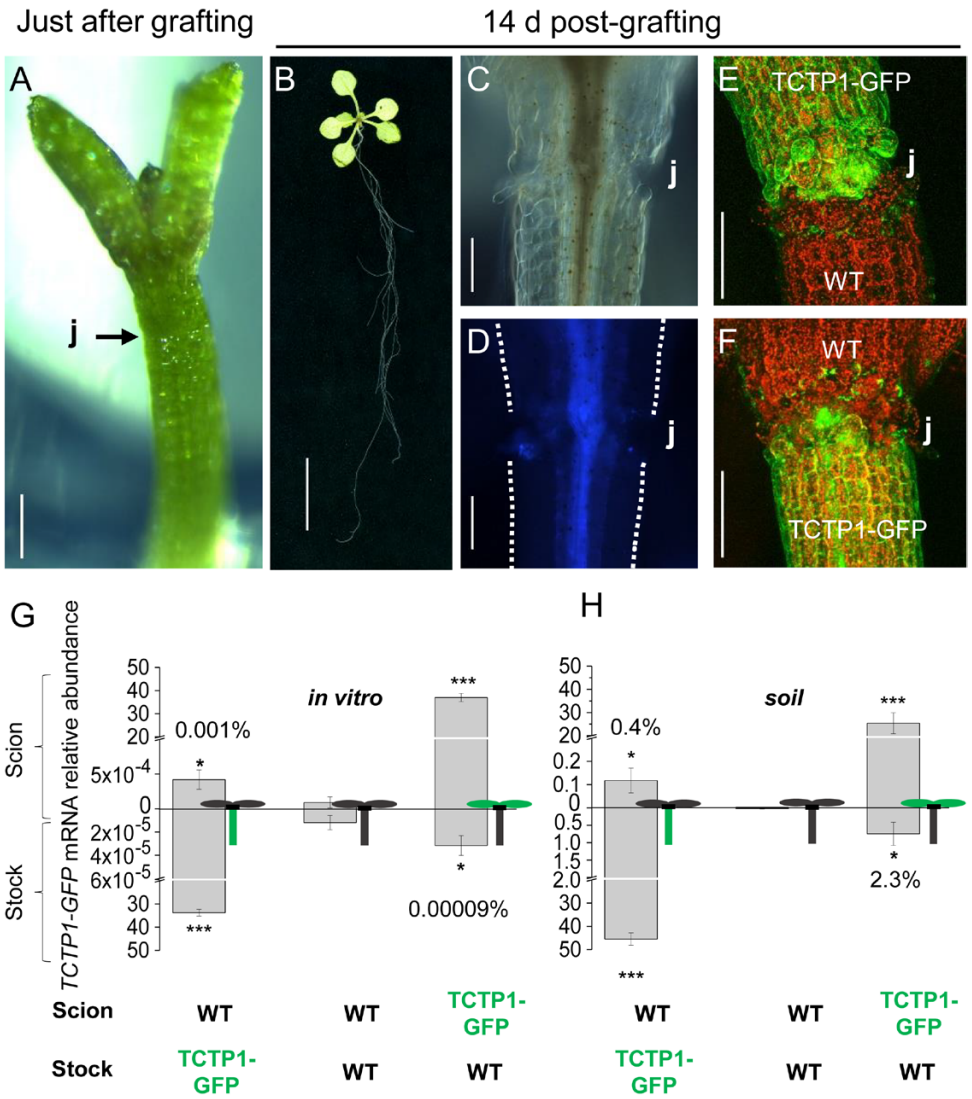

Fig. 1. AtTCTP1 mRNA moves over hypocotylar graft junctions in young and adult plants, in variable proportions. (A–D) Representative images of: scion–rootstock junction (j) immediately after grafting (A); whole seedling (B) and graft junction (C and D) 14 DAG. DIC image (C) and autofluorescence image (D). Scale bars, 250 μm (A), 10 mm (B), 200 μm (C and D). (E and F) TCTP1–GFP fluorescence at the graft junction imaged by confocal microscopy. WT root grafted to a *pTCTP1::gTCTP1-GFP* scion (E) and a WT scion grafted to a *pTCTP1::gTCTP1-GFP* root (F). Scale bar, 200 μm. (G and H) *AtTCTP1-GFP* and endogenous *AtTCTP1* transcripts were quantified by qRT–PCR in the scion (values above the *x*-axis) and rootstock (values below the *x*-axis) of reciprocal grafts between WT and transgenic *pTCTP1::gTCTP1-GFP* seedlings grown *in vitro* and sampled at 14 DAG (G) or transferred to soil 10 DAG and sampled at 80 DAG (H). Scion–rootstock combinations are indicated below each panel, and schematized beside each bar. Values are means ±SE of fold change in target gene expression relative to expression of four reference genes (*in vitro* seedlings, $n=5$ biological replicates each consisting of pooled rosettes or rootstocks from five plants; soil-grown plants, $n \geq 6$ biological replicates, each consisting of pooled rosettes or rootstocks from two plants). Asterisks denote statistically significant expression differences compared with the WT/WT control homograft by one-tailed Student's *t*-test (*$P<0.05$; ***$P<0.001$). Similar results were obtained with two sets of GFP-specific primers as listed in the Materials and methods. The percentages above or below bars denote the abundance of mobile *AtTCTP1-GFP* transcripts measured in WT/TCTP1–GFP and TCTP1–GFP/WT grafts relative to the total amount of *AtTCTP1-GFP* transcripts produced by the *TCTP1-GFP* scion or rootstock, respectively, in the two sets of heterografts.

of *AtTCTP1-GFP* transcripts produced (0.4% and 2.3% of shootward and rootward mobile *AtTCTP1-GFP* transcripts in WT/TCTP1–GFP and TCTP1–GFP/WT, respectively, in soil-grown plants; 0.001% and 0.00009%, respectively, in seedlings raised on agar media). These data demonstrate sustained bi-directional mobility of *AtTCTP1* mRNA, of variable magnitude, in both the shootward and rootward direction.

AtTCTP1 protein of scion origin is detected in WT rootstock, with preferential accumulation in pericycle cells at sites of lateral root formation

We next examined the presence of the encoded TCTP1–GFP protein in these grafts by confocal laser microscopy. A weak TCTP1–GFP fluorescence signal was consistently detected in the primary root of *pAtTCTP1::gTCTP1-GFP/WT* heterografts (Fig. 2A–E), whether in the agar-grown seedlings (Fig. 2A–C, 8–13 DAG) or the older soil-grown plants (Fig. 2E; 80 DAG). Imaging the scion with the same microscope settings completely saturated the confocal photomultiplier (images therefore not shown). GFP fluorescence localized along the vascular strands, with acropetally increasing intensity towards the root tip, down to ~250 μm from the quiescent centre (251±11.8 μm at 13 DAG, n=5); that is, within the transition zone from the root elongation zone to the root meristem, where the GFP signal completely disappeared (Fig. 2A, B, E; Supplementary Fig. S1 at *JXB* online), coinciding with the end of the protophloem. Closer inspection at higher resolution along the root elongation and differentiation zones showed patchy GFP signal intensity, reflecting preferential protein accumulation in pericycle cells at the sites of LR initiation (Fig. 2C, F, G). WT roots grafted to scions expressing a *p35S::YFP-cTCTP1* construct providing a much stronger fluorescence signal, also clearly showed pericycle-specific localization of YFP fluorescence (Fig. 2D). TCTP1–GFP fluorescence was also detected in LRPs, but was much weaker, sometimes barely detectable, until the root had emerged and started to elongate rapidly (Fig. 2H). The pattern of GFP fluorescence in control roots grafted on a scion expressing GFP alone under the same promoter was very different, with a very high ubiquitous signal in the whole stele and throughout the root meristem (Supplementary Fig. S2), as previously reported (Stadler *et al.*, 2005; Ross-Elliott *et al.*, 2017). Taken together, these results suggest that rootward *TCTP1* mobility is actively controlled and may have a specific signalling function in root development, targeted to cells involved in the spatial patterning of LRPs along the primary root.

To examine this in more detail, we monitored the appearance of TCTP1–GFP fluorescence in the rootstock of TCTP1–GFP/WT grafts over a 10 d period following grafting. The earliest evidence of GFP fluorescence was on 7 DAG (23 out of 28 roots; Supplementary Fig. S3), consistent with reports of establishment of a fully functional graft junction in Arabidopsis (Melnyk *et al.*, 2015). Strikingly, the preferential TCTP1–GFP accumulation in the primary root elongation zone observed in older roots (Fig. 2) was already obvious (Fig. 3A). Moreover, when imaging the entire root from base to tip, TCTP1–GFP fluorescence was first encountered in two patches localized in pericycle cells at the base of the two youngest LRPs, at both initiation stages I and II (Malamy and Benfey, 1997) (Fig. 3H, I). This result further supports the notion of a destination-selective signalling function of mobile *TCTP1* gene products originating from the shoot, in the initiation of LRs. Given the bi-directional mobility of *TCTP1* mRNA (Fig. 1G, H), we examined the presence of GFP fluorescence in WT scions grafted onto *pAtTCTP1::gAtTCTP1-GFP* roots. GFP fluorescence was undetectable, whether in young or mature leaves, or in the shoot apical meristem (Fig. 2I, J).

Constitutive expression of AtTCTP1 *in scion promotes scion growth which in turn stimulates root growth*

In our earlier characterization of *AtTCTP1*, we showed that *AtTCTP1* gene products, mRNA and protein, are constitutively highly expressed in the primary root meristem and LRPs, and that *AtTCTP1* silencing inhibits root elongation and LR branching (Berkowitz *et al.*, 2008). The above results in the present study suggested a role for AtTCTP1 also in root development through mobility. To investigate that, due to lack of roots devoid of constitutive *AtTCTP1* expression given the embryo lethality of total *AtTCTP1* knock-out and the dwarfism of *tctp1* seedlings rescued through embryo culture (Berkowitz *et al.*, 2008; Brioudes *et al.*, 2010), we severed TCTP1-RNAi roots from 5-day-old seedlings expressing a constitutive *AtTCTP1* silencing construct (Berkowitz *et al.*, 2008) (hereafter referred to as TCTP1-RNAi or RNAi), and grafted them to either a WT scion of the same age, or to a homologous TCTP1-RNAi scion. Root development in these grafts was then monitored over the next 3–4 weeks. We reasoned that the 100-fold higher *AtTCTP1* constitutive expression in WT scions than TCTP1-RNAi scions (Berkowitz *et al.*, 2008) should translate into a significantly increased amount of scion to root mobile *AtTCTP1* mRNA and protein in WT/RNAi compared with RNAi/RNAi grafts, and thus enable us to determine whether the distinctive short root and reduced branching of the rootstock is root autonomous or involves signalling by *AtTCTP1* from the scion. WT/RNAi reciprocal heterografts were grown alongside each other and control WT/WT and RNAi/RNAi homografts, in replicated plates. WT primary roots grew faster than TCTP1-RNAi roots irrespective of scion genotype (Fig. 4A, B). Both WT and TCTP1-RNAi roots elongated faster when grafted onto a WT rather than a TCTP1-RNAi scion (26% and 21% increase in maximum relative elongation rate at 13 DAG, respectively; Fig. 4C). It is known, however, that siRNA can move long distances through the plant (Molnar *et al.*, 2010; Bai *et al.*, 2011; Melnyk *et al.*, 2011; Liang *et al.*, 2012). To test whether this explained the root growth inhibition associated with TCTP1-RNAi scions, we measured *AtTCTP1* transcript abundance in homo- and heterograft scions and rootstocks by qRT–PCR. *AtTCTP1* mRNA levels in WT roots showed a nearly 6-fold reduction in RNAi/WT seedlings compared with WT/WT seedlings (P=0.005; Fig. 4D). This is much higher than could be expected from simply a reduction of mobile rootward *AtTCTP1* mRNAs (see Fig. 1G, H) and hence suggested some down-regulation of *AtTCTP1* expression in these roots by mobile siRNA from the RNAi

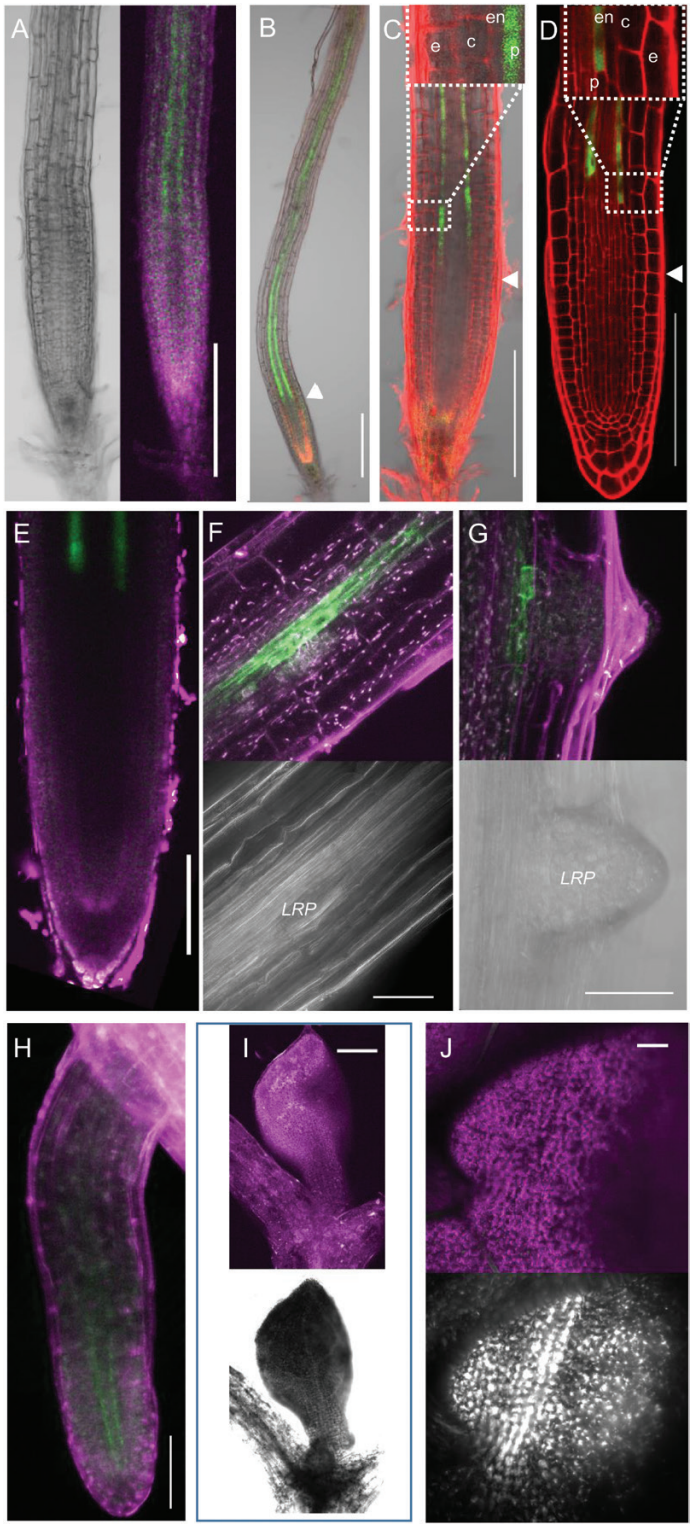

Fig. 2. Distinctive pattern of TCTP1–GFP fluorescence in WT rootstock grafted to TCTP1–GFP scions, with preferential accumulation in pericycle cells at sites of lateral root formation. (A–H) Confocal laser microscopy images of WT roots grafted onto scions expressing *pTCTP1::gTCTP1-GFP* (A–C and E–H) or *p35S::cYFP-TCTP1* (D). Roots were imaged in seedlings grown in agar plates, 8 DAG (A) or 13 DAG (B–D) ($n \geq 30$ primary roots), and in flowering soil-grown plants, 80 DAG (E–H), $n \geq 10$; primary root and LRPs (E–G); elongating lateral root (H). Note the localization of the GFP fluorescence in parallel strands, the increasing signal closest to the root tip, and the preferential accumulation of the GFP-tagged TCTP1 protein in pericycle cells (C, D and F, G) at the sites of lateral root initiation (labelled *LRP* in F and G). GFP fluorescence (green) and autofluorescence (magenta/red) were separated by spectral unmixing. Arrowheads in (B–D) denote the boundary between root meristem, transition zone, and elongation zone only of the root. Inserts in (C) and (D) show TCTP1–GFP (C) and YFP–TCTP1 (D) localization, respectively, in the pericycle (p); GFP fluorescence was undetectable in the epidermis (e), the endodermis (en), or the cortex (c). (I and J) Absence of detectable GFP fluorescence signal in WT scions grafted to *pTCTP1::gTCTP1-GFP* roots, 8 DAG in agar-grown plants (I) or 80 DAG in soil-grown plants (J). Scale bars=200 μm except in (J) 100 μm. Given the low-intensity GFP signal when *TCTP1-GFP* expression in the scion is driven by the native *AtTCTP1* promoter, imaging had to be done at low magnification and larger pinhole aperture (×10 and 4.5 AU, respectively; A–C and I–H), limiting resolution, in contrast to roots grafted onto *p35S:cTCTP1-GFP* (×63, 1 AU, D).

scion. In contrast, *AtTCTP1* transcript abundance in RNAi roots was similar regardless of scion genotype (0.68±0.118 and 0.77±0.013 relative transcript abundance in RNAi/RNAi and WT/RNAi grafts, respectively, P=0.55; Fig. 4D), ruling out that simple explanation for their slower elongation rate. To verify that mobile *AtTCTP1* transcripts from the scion were not silenced by siRNA upon delivery to the root, we grafted TCTP1–GFP scions on TCTP1-RNAi roots and quantified transgenic *TCTP1-GFP* mRNAs in the rootstock (Fig. 4E). *TCTP1-GFP* mRNAs were present in roots of TCTP1–GFP/RNAi grafts, in low but significant abundance, representing ~0.006% of scion total *TCTP1-GFP* mRNAs, that is in fact a similar or even higher proportion than found in WT rootstocks of TCTP1–GFP/WT grafts in our earlier experiments, under similar conditions (e.g. Fig. 1G). This result shows that a significant amount of *AtTCTP1-GFP* transcripts translocated from the scion to RNAi rootstock escaped silencing. GFP fluorescence from the encoded TCTP1–GFP protein was also consistently detected, with the same distinctive spatial expression pattern (Fig. 4F compared with Fig. 2B). These results suggest the presence of a larger amount of intact *TCTP1* gene products of scion origin in TCTP1-RNAi roots grafted to a WT scion instead of a homologous TCTP1-RNAi scion. The low abundance of translocated *TCTP1-GFP* transcripts compared with the high abundance of native root endogenous *TCTP1* transcripts is consistent with the only small change in total *TCTP1* transcript abundance measured earlier in rootstocks of WT/RNAi grafts compared with RNAi/RNAi grafts (Fig. 4D).

Despite all being trimmed to a similar size at the time of grafting (see the Materials and methods), WT scions quickly became larger than TCTP1-RNAi scions (Supplementary Fig. S4), consistent with the high expression of *AtTCTP1* in the shoot apical meristem and its growth-promoting effect in leaves (Berkowitz *et al.*, 2008). This suggested that the faster elongation rates of TCTP1-RNAi roots in WT/RNAi than in RNAi/RNAi grafts might then at least partly reflect an increased photoassimilate supply from larger scions, rather than higher abundance of *AtTCTP1* mRNA translocated from the scion. To address this, we grafted TCTP1-RNAi roots onto WT scions or onto homologous TCTP1-RNAi scions of the same age as earlier. However, at 7 DAG, when the graft junction was fully established and TCTP1-RNAi root lengths were still similar regardless of scion genotype (12.8±1.25 mm and 11.4±0.91 mm

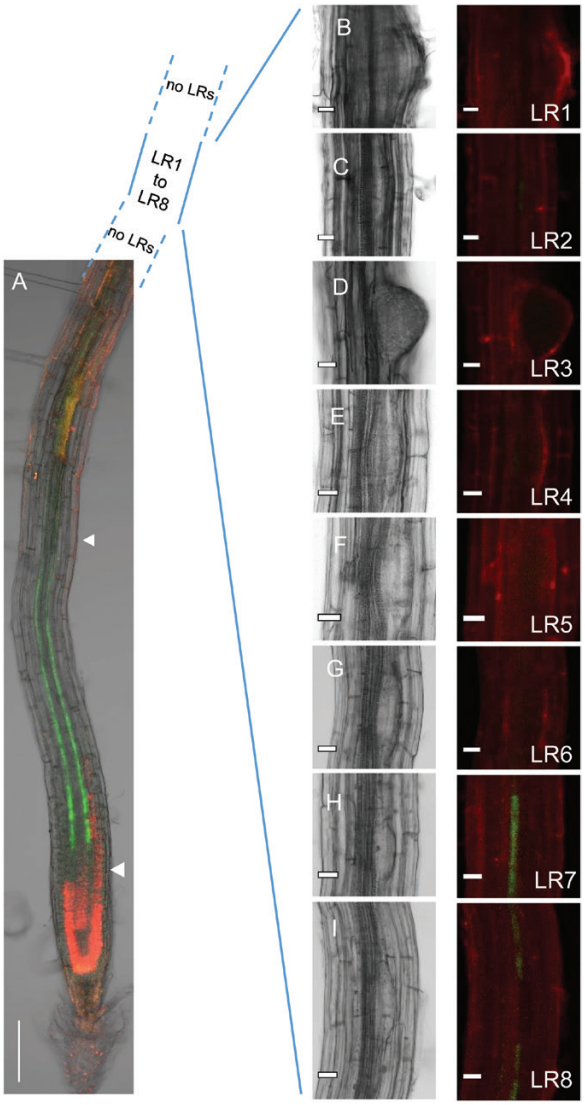

Fig. 3. Scion-derived TCTP1–GFP fluorescence in grafted WT rootstocks is first detected at the most apical lateral root initiation sites. (A) Confocal laser scanning microscopy image of a WT primary root grafted to a scion expressing *pTCTP1::gTCTP1-GFP*, 7 DAG. Scale bar, 200 µm. Arrowheads denote the boundaries between root meristem, elongation zone, and differentiation zone. (B–I) Confocal laser-scanning microscope images of lateral root primordia along the primary root, from the most distal (B) to the most apical primordium (I) closest to the root tip, just above the zone of LRP priming. For each primordium, the transmission channel is on the left and the fluorescence channel is on the right. TCTP1–GFP fluorescence (green) is only visible at the initiation sites of the two youngest LRPs (H and I). Scale bars, 20 µm.

in WT/RNAi and RNAi/RNAi grafts, respectively; P=0.13; Fig. 4B), we normalized WT scion sizes to RNAi scion sizes, via tip amputation of leaf 1 (scions hereafter denoted WT_{AMP}). To minimize potential confounding wounding effects in subsequent phenotypic analyses, one of the tiny remaining stumps of the two cotyledons cut out 7 d earlier at the time of grafting was manually pinched in control grafts, at its very tip, causing a similar very brief and spatially restricted micro-wounding event in all scions. Over the next 1 and 2 weeks, scion sizes were still similar in the two sets of grafts (WT_{AMP}/RNAi and RNAi/RNAi; Fig. 4G; Supplementary Fig. S5A), and much smaller than non-amputated WT scions in WT/RNAi grafts (~2-fold difference at 22 DAG; Fig. 4G). Remarkably, associated TCTP1-RNAi rootstocks showed similar primary root lengths (Fig. 4H, I: Supplementary Fig. S5B), significantly shorter than roots of WT/RNAi grafts. When individually plotted against scion sizes, root lengths described a unique relationship for the three sets of grafts, and data points for TCTP1-RNAi roots associated with WT_{AMP} or TCTP1-RNAi scions overlapped (Fig. 4H). Consistently, relative root elongation rates over the monitoring period (7–22 DAG) were similar (4.17±0.15 h^{-1} and 4.07±0.14 h^{-1} in WT_{AMP}/RNAi and RNAi/RNAi grafts, respectively, P=0.09). Moreover, the cell length profiles in the root elongation zone also showed complete overlap, and final cell lengths were similar (Fig. 4J). These results indicate that, at the same scion size, differences in constitutive *AtTCTP1* expression levels in the scion and rootward mobile *AtTCTP1* gene products have little impact on primary root elongation during early post-embryonic development.

Graft-mobile AtTCTP1 *transcripts and encoded protein promote lateral root initiation and emergence*

As scion-derived TCTP1–GFP showed preferential accumulation at sites of LR initiation (Fig. 2), we next closely examined root branching patterns. The number of LRs varied between plants. That variation was closely correlated to variation in scion size (Fig. 5A). Data points for WT_{AMP}/RNAi and WT/RNAi grafts fell on the same line (slopes 0.38±0.02 and 0.36±0.04, respectively), indicating that partial amputation of WT_{AMP} scions *per se* had no unwanted confounding effects on root development. Remarkably, LR numbers in RNAi/RNAi grafts fell significantly below those counted in WT_{AMP}/RNAi heterografts. The density of LR formation sites along the primary root was decreased by 41% on average (Fig. 5B), while being as high in roots grafted to WT_{AMP} rather than much larger WT scions (P=0.36; Fig. 5B).

We next used DIC microscopy to examine the entire length of the primary root in WT_{AMP}/RNAi and RNAi/RNAi grafts, for non-emerged LRPs (stages I–VII; Malamy and Benfey, 1997) in addition to emerged LRs, also separately scoring those found on the primary root segment formed pre- or post-grafting and scion size normalization (Fig. 5C). The former were confined to the basal 8–9 mm of the primary root, and in total amounted to 2.9 on average in the two sets of grafts (P=0.89). The density of both non-emerged LRPs and emerged LRs on the younger, proximal primary root segment formed post-scion size normalization was significantly greater in WT_{AMP}/RNAi than RNAi/RNAi grafts (P<0.05; Fig. 5C, D). This was already clear at 12 DAG and even more obvious 6 d later. Consistent with the increased LRP density, the expression of *CycB1;1*, a marker of the early divisions of pericycle cells that initiate LR formation (Beeckman *et al.*, 2001), was also increased in roots from WT_{AMP}/RNAi grafts compared with those of RNAi/RNAi grafts (P<0.004; Fig. 5E). In the course of these experiments, we noticed that the youngest, most acropetal LRPs seemed to be located closer to the root tip in those grafts. Systematic measurements of its coordinate along the primary root showed that the zone of LR formation indeed

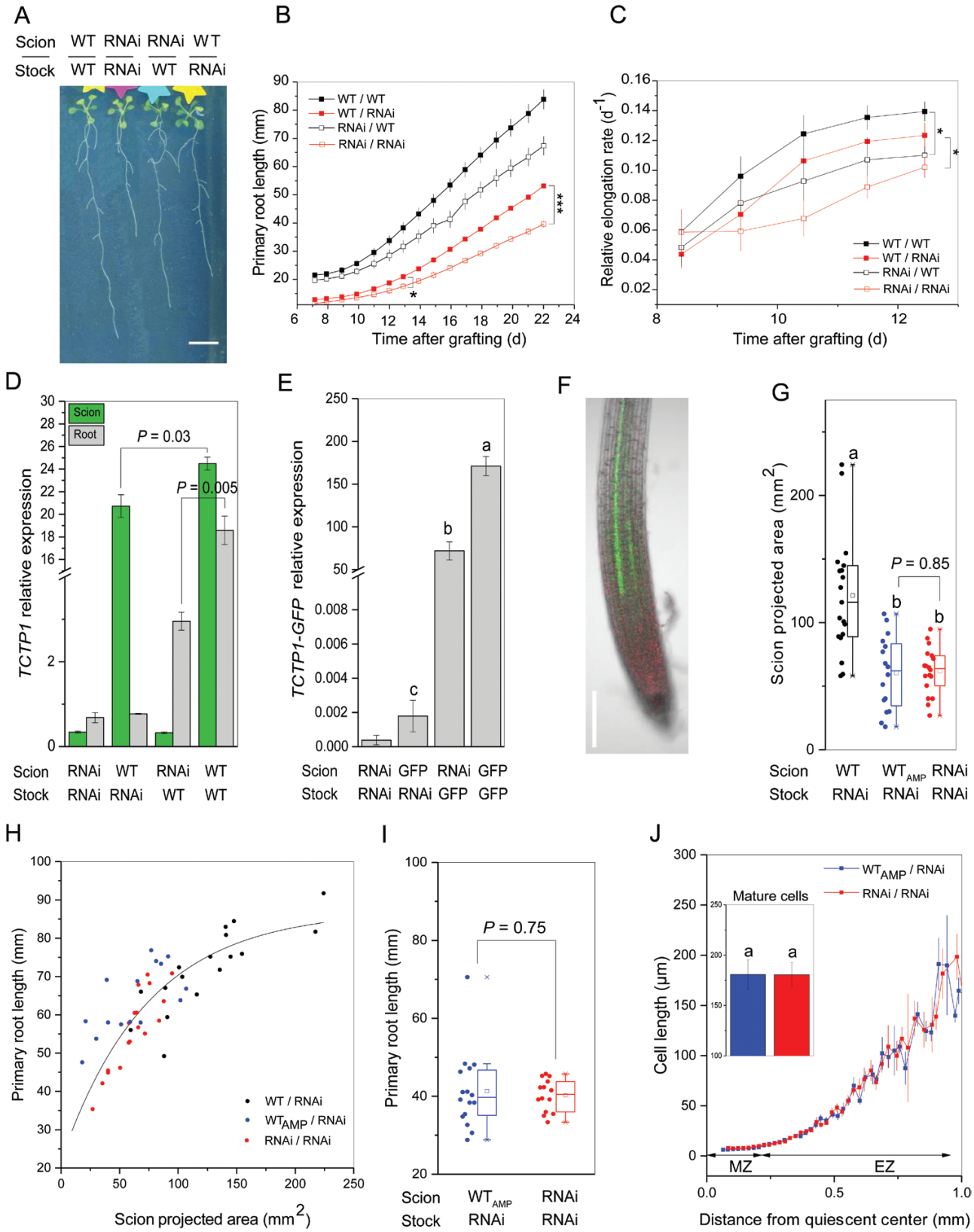

Fig. 4. Constitutive expression of *AtTCTP1* in the scion promotes scion growth which in turn stimulates primary root elongation. (A) Representative images of reciprocal grafts between WT and TCTP1-RNAi lines, and control WT/WT and TCTP1–RNAi/TCTP1-RNAi homografts, 22 DAG. Scale bar, 10 mm. (B and C) Primary root lengths (B) and relative root elongation rates (C) versus time. Means ±SE, n=6–9. (D) *AtTCTP1* relative gene expression levels in rootstocks and scions, 22 DAG (means ±SE, n=3 pools of at least five plants each). (B and C) Asterisks denote statistically significant differences by two-tailed Student's t-test; *P<0.05; **P<0.01; ***P<0.001. (E) *AtTCTP1-GFP* relative expression in the rootstocks of reciprocal grafts between *TCTP1-RNAi* and *TCTP1-GFP* lines (denoted for brevity 'RNAi' and 'GFP', respectively, in the figure), and control homografts. Different letters indicate statistically significant differences from noise levels in roots from RNAi/RNAi grafts by one-way ANOVA followed by Tukey's post-hoc test, n=4 pools of

extended significantly closer to the root meristem in WT_{AMP}/RNAi than RNAi/RNAi grafts ($P=4\times10^{-4}$; Fig. 5F). Root patterning was completely normal, however (Supplementary Fig. S6). Taken together, these data indicate a stimulation of LR initiation and emergence in WT_{AMP}/RNAi grafts, at the same scion size and primary root length and anatomy, thus probably being related to enhanced delivery of mobile *AtTCTP1* gene product(s) from WT scions compared with RNAi scions. The identical cell length profiles along the whole transition, elongation, and differentiation zones of the two sets of roots imply an increased frequency of LR priming events along the primary root pericycle.

While initiated and emerging in greater number in WT_{AMP}/RNAi than RNAi/RNAi grafts, LRs were on average shorter ($P=4\times10^{-4}$; Fig. 5G). Strikingly, the overall result was that their cumulated length over the whole primary root was unaffected, similar to that measured for RNAi/RNAi grafts ($P=0.32$; Fig. 5H; Supplementary Fig. S7). Plant to plant variation of cumulated LR root length was correlated to individual variation in scion size (Fig. 5H), as found for primary root length, and data points fell on the same relationship for the two sets of grafts (Fig. 5H). Taken as a whole, these results indicate a signalling role for *AtTCTP1* rootward mobility in root development, specifically targeted at the regulation of early events of LR formation and of LRP emergence from covering layers.

Discussion

TCTP function and physiological roles in plants are only beginning to be unravelled. The possibility of a dual role, as a protein acting not only cell autonomously, but also extracellularly as found in mammals and other eukaryotes, remains unknown. This study indicates a targeted, selective function of scion-encoded mobile endogenous Arabidopsis *AtTCTP1* mRNA and translated protein in shaping the deployment of the root system.

AtTCTP1 mRNA movement was reported to occur in a strictly rootward direction (Thieme *et al.*, 2015). Here, we consistently detected a bi-directional movement, whether in plate assays with young seedlings raised under similar conditions to those in the earlier study, or after graft transfer to soil. This discrepancy may be related to the different reporter constructs used: full genomic *TCTP1* here, including the 5'-untranslated region (UTR) and native upstream promoter region; *TCTP1* cDNA was fused to the constitutive *Cauliflower mosaic virus* promoter in the previous study. The 5'-UTR of *AtTCTP1* contains a conserved 5'-TOP (terminal oligopyrimidine tract) motif, and two AUUUA motifs are present in the 3'-UTR. TOP mRNAs are highly sensitive to translational control, and AUUUA motifs are also important in mRNA stability and translation (Barreau *et al.*, 2005). In animals, these motifs are thought to be important in the control of TCTP translation (Bommer and Thiele, 2004), and in Arabidopsis itself have been suggested to influence the expression pattern of AtTCTP1 (Brioudes *et al.*, 2010). It may be that the 5'- and 3'-UTRs also play a role in the mobility and/or transport of *AtTCTP1* transcripts, as shown for *StBEL5* mRNA movement from leaf and petioles to stolon tips in the regulation of tuber formation in *Solanum tuberosum* (Banerjee *et al.*, 2009). Supporting our results, a bi-directional endogenous movement of the native *Vitis vinifera TCTP1* mRNA homologous to *AtTCTP1* has also been documented in heterografts of two polymorphic *Vitis* genotypes, through genome-wide sequencing of scions and rootstock mRNAs (Yang *et al.*, 2015).

The consistency of our observations in seedlings grown *in vitro* and older soil-grown plants provides evidence that long-distance movement of endogenous *AtTCTP1* mRNA between the shoot and root is not a transient occurrence, nor an experimental artefact, but a sustained phenomenon, which takes place under physiological conditions.

If that phenomenon has a physiological function, one would expect it to be actively controlled, in a growth condition- or development stage-dependent manner. Fitting with this, while always representing a small fraction of the transcripts produced in the source organ as seems the norm (Notaguchi *et al.*, 2015; Yang *et al.*, 2015; Morris, 2018), the proportion of At*TCTP1* mRNAs transmitted across root–shoot graft junctions showed significant variation from plant to plant and between *in vitro* and soil experiments (Fig. 1). Consistently, for rootward movement, the fluorescence signal associated with TCTP1–GFP protein derived from mobile scion *TCTP1* mRNAs was also of variable intensity, especially in the population of elongating LRs of soil-grown plants, even being undetectable in some. No conclusion is possible about TCTP1–GFP protein in the scion of reciprocal WT/TCTP1–GFP grafts. The fact that its presence was not detected in our experiments could indicate absence of translation under our experimental conditions—TCTP proteins are notoriously sensitive to translational control, as reflected in their name—or very low abundance, below the limits of detection, but nevertheless could have functionality as found for other regulatory proteins of root development, such as BREVIS RADIX (Mouchel *et al.*, 2004).

Another expectation of mobile gene products serving a physiological function is that they give rise to distinct, quantifiable phenotypes. To examine this, we focused on *AtTCTP1* rootward mobility. Our results provide convergent evidence towards a systemic signalling role targeted at cells involved in the initiation and emergence of LRs. First, the scion-derived TCTP–GFP protein detected in the WT primary root of

≥6 roots). (F) Representative image of GFP fluorescence in TCTP1-RNAi roots grafted to TCTP1–GFP scions. Scale bar, 200 µm. (G–J) Comparison of grafted seedlings sharing the same rootstock (TCTP1-RNAi) but differing in scion genotype or size ('AMP' subscript denotes WT scions trimmed 7 DAG; see the Materials and methods): (G) scion sizes 22 DAG; (H) individual primary root lengths versus scion projected area, 22 DAG; (I) primary root lengths, 18 DAG in an independent experiment. (G–I) Dots represent individual seedlings, n=14–19 seedlings per graft type; boxes show median, first, and third quartiles, and upper and lower whiskers give a graphic representation of the interval containing all data points within ± [1.5×(Q_3–Q_1)] range. (J) Epidermal cell lengths along the primary root meristem (MZ) and elongation zone (EZ), n=5 roots per graft type. Shown are moving averages of cellular lengths over 20 µm windows. The inset depicts mature cell lengths (means ±SE). Different letters in (G), (I), and (J) denote statistically significant differences by one-way ANOVA (G) or Student's t-test (I, J) ($P<0.05$ unless indicated).

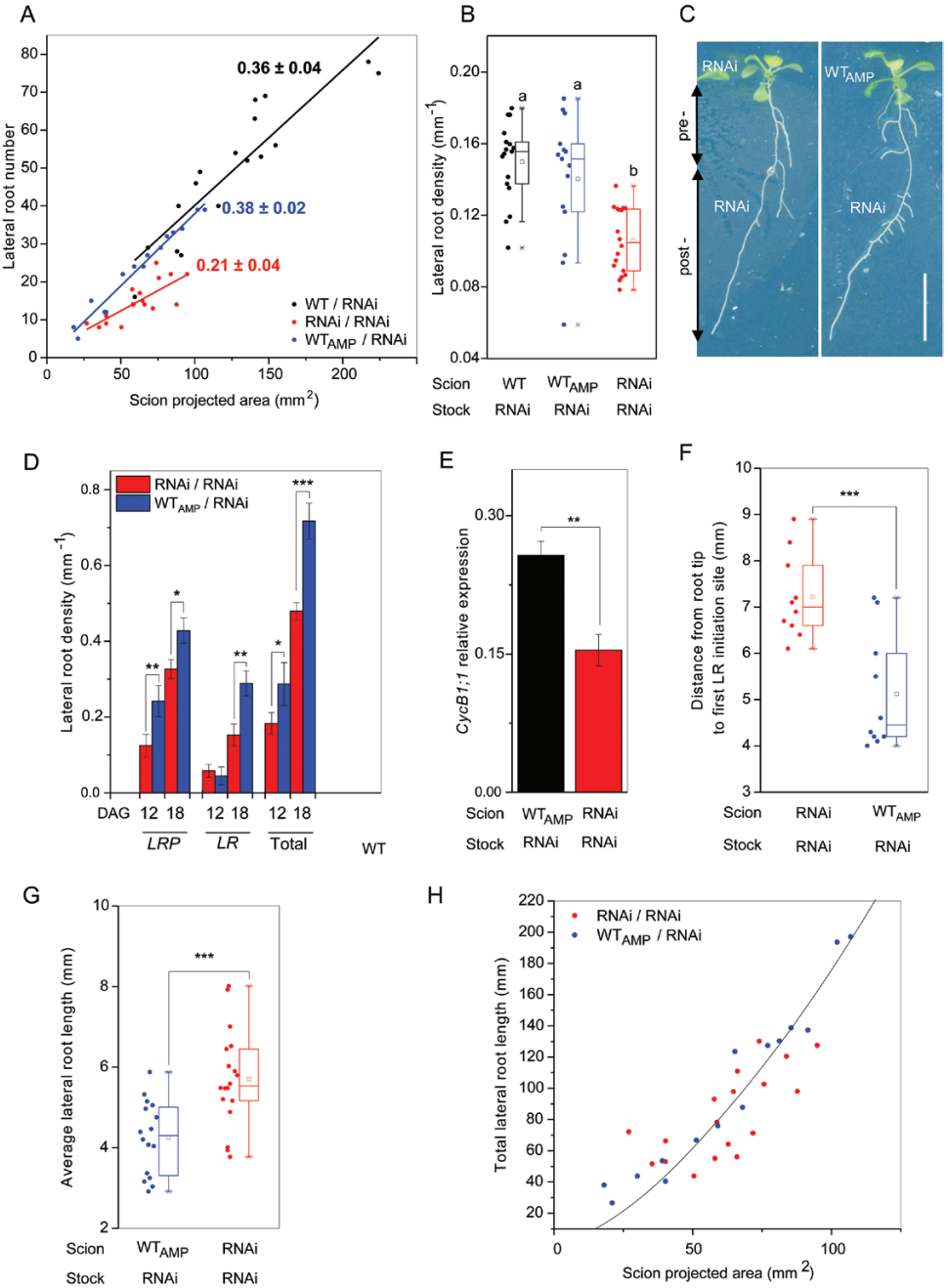

Fig. 5. Rootward TCTP1 movement promotes lateral root initiation and emergence. (A) Lateral root number as a function of scion projected area; linear regression lines and slopes ±SE are shown for each set of grafts, *n*=15–17. (B) Lateral root density (number of lateral roots per unit length of primary root). Different letters indicate statistically significant differences by one-way ANOVA followed by Bonferroni post-hoc test; *n*=15–17 roots. (C) Representative photographs of a TCTP1-RNAi/TCTP1-RNAi homograft (left) and a WT_{AMP}/TCTP1-RNAi heterograft (right), 18 DAG: 'pre-'and 'post' denote the portions of primary root formed pre- and post-grafting and scion size normalization (0–8 mm and 10 mm to root tip, respectively). Scale bar, 10 mm. (D) Lateral root density on the primary root portion formed after scion size normalization. *LRP* and *LR* denote non-emerged lateral root primordia and elongating lateral roots, respectively. Means ±SE, *n*=14 roots. (E) *Cyclin B1;1* relative expression measured by qRT–PCR in rootstocks sampled 10 DAG. Means ±SE, *n*=4 biological replicates, each consisting of at least six pooled rootstocks. (F) Distance between the youngest, most proximal LRP and the root tip, *n*=10. (G) Average lateral root length, and (H) total lateral root length as a function of scion projected area, measured 18 DAG. (D–G) Statistical significance was determined by two-tailed Student's *t*-test (**P*<0.05; ***P*<0.01; ****P*<0.001, *n*=14–18). In (A), (B), (G), and (H), each data point represents an individual plant.

TCTP1–GFP/WT grafts consistently showed a distinctive localization pattern, being (i) absent from the root meristem; (ii) confined to the vasculature, with recurrent peaks of higher intensity, systematically coinciding with sites of LRP initiation in the pericycle; and (iii) highly abundant in the root elongation and transition zones upstream of the root meristem proper, which encompass a region of 'oscillatory gene expression' where priming of LR initiation takes place (De Smet *et al.*, 2007; Moreno-Risueno *et al.*, 2010). This pattern is in stark contrast to the ubiquitous expression, in all root layers and also the root meristem, of the constitutive root AtTCTP1 protein, translated from locally transcribed *AtTCTP1* transcripts

(Berkowitz *et al.*, 2008). It is also distinct from the pattern observed for mobile GFP or YFP alone, and passive mass flow transport through the phloem and leakage from companion cells to pericycle cells. These results indicate the presence of active targeting, capture, or unloading mechanisms in the root of *AtTCTP1* gene products encoded in the shoot. Secondly, TCTP1-RNAi roots of similar structure, anatomy, size, and elongation rate, but associated with WT_{AMP} scions rather than TCTP1-RNAi scions of similar size, exhibited an extended zone of LR formation starting closer to the root tip. Thirdly, the densities of root branching sites (emerged LRs) and of LR initiation sites (non-emerged LRPs at more acropetal positions) along that zone were both increased. The specificity of these changes and the shift towards more numerous and on average shorter LRs, in an extended zone, while the overall length of root over the whole root system was unaffected, contrasts with the general promotion of both primary root and LR elongation associated with increased local constitutive AtTCTP1 expression (Berkowitz *et al.*, 2008), with increased scion size (Figs 4, 5), or with independently induced increases of photoassimilate supply via stimulation of carbon metabolism (Freixes *et al.*, 2002; Lee-Ho et al., 2007). Differential sucrose uptake by TCTP1-RNAi and WT_{AMP} scions directly from the medium—which is known to influence LR emergence (MacGregor *et al.*, 2008)—can also be ruled out as an explanatory factor for the effects of scion genotype observed here on root system architecture, as our grafts were raised in the absence of exogenous sucrose supply.

The phloem is the long-distance delivery path to the roots of auxin synthesized in leaves and cotyledons. Auxin has a pivotal role in orchestrating root architecture (Laskowski *et al.*, 2008; Lewis *et al.*, 2011; Raya-González *et al.*, 2012), being required for the activation of LR potential initiation sites in the pericycle, the subsequent process of primordium initiation and formation, and the breaking of overlying tissues for its emergence out of the primary root epidermis (Casimiro *et al.*, 2001; De Smet *et al.*, 2007, 2010; Dubrovsky *et al.*, 2008; Peret *et al.*, 2009, 2012; De Rybel *et al.*, 2010; Muraro *et al.*, 2013). However, TCTP1-RNAi seedlings of the same age as used in this study and raised under similar growth conditions in earlier experiments were in fact found to have higher endogenous auxin concentrations than WT seedlings, in both shoots and roots (Berkowitz *et al.*, 2008), and, consistently, higher expression of the auxin-inducible transcriptional regulator IAA5. In addition, application of the auxin polar transport inhibitor NPA in the present study had no detectable influence on the abundance or localization of the AtTCTP1 protein translated from mobile *AtTCTP1* transcripts (Supplementary Fig. S8). It is therefore unlikely that stimulation of LR initiation and emergence in WT_{AMP}/RNAi compared with RNAi/RNAi grafts could result from a higher auxin production in the scion and increased auxin delivery to the root.

Taken as a whole, these observations provide a compelling argument for ascribing the scion genotype-dependent modulation of root architecture observed in our grafts to a differential transmission rate of mobile scion *AtTCTP1* gene products to the root, associated with the large (two orders of magnitude) difference in constitutive *AtTCTP1* transcript abundance between WT_{AMP} and TCTP1-RNAi scions (Fig. 4D; Berkowitz *et al.*, 2008). We propose a model (Fig. 6) where local constitutive *AtTCTP1* controls core cellular processes, vital to cellular function, growth, and proliferation in both roots and shoot, and determines the overall length of root that can be formed, in interaction with photoassimilate supply. Mobile *AtTCTP1* mRNAs—and perhaps proteins—transmitted from the shoot act as destination-selective systemic signalling molecules to modulate the spatio-temporal pattern of LR initiation and emergence dynamically, and possibly too the initial priming of pericycle LRP founder cells (i.e. the plasticity of root system architecture).

Whether *AtTCTP1* mRNAs are only transmitted from shoot to roots, and fulfil their function through destination-selective delivery and decoding in the root, or whether some might be translated in the scion, followed by selective loading of the protein into the phloem, and selective unloading in specific destination cells in the root, remains to be determined. The two scenarios are not exclusive. Disentangling them will be challenging given the high and ubiquitous constitutive expression of AtTCTP1 in source and destination tissues of mobile *AtTCTP1* mRNAs, and also the limitations of transgenic approaches with non-endogenous gene products when it comes to characterization of movement and function. Also suggesting the possibility of AtTCTP1 protein mobility, an actively controlled rootward movement of the highly similar pumpkin CmTCTP1 (CmaCh11G012000) in rice phloem sieve tubes has been reported (Aoki *et al.*, 2005). Its functionality was not analysed but, most interestingly, the mobile CmTCTP1 (CmaCh11G012000) was found to be translocated as part of a protein complex including CmPP16-1 and CmPP16-2 phloem RNA-binding proteins and also the initiation factor CmeIF5A, among other undetermined components; an association fitting with the assumed molecular function of plant TCTPs in protein synthesis, as established in animals (Cans and Passer, 2003; Wu *et al.*, 2015). Under either scenario—mobility of the messenger only, or also of the protein—it will be intriguing to elucidate how destination cells recognize the mobile *AtTCTP1* gene products generated in distant cells from those they autonomously produce, and what their mechanisms of action are.

The plasticity of root system architecture is pivotal to plant adaptation to changes in environmental conditions, and strategic mining of spatially and temporally variable soil resources. *AtTCTP1* appears as a central controller of that plasticity. Combining a dual function, namely as a general constitutive growth promoter and a mobile signalling agent between shoot and roots, in a vital, highly expressed gene, furthermore encoding a protein highly sensitive to translational and post-translational modifications, appears to be a clever strategy for a sensitive and dynamic tuning of root system architecture to optimize the compromise for roots between reaching deeper or branching more profusely depending on growth conditions. Interestingly, the much lower and more specifically expressed Arabidopsis *AtTCTP1* orthologue, *AtTCTP2*, was reported to encode an mRNA and protein with bi-directional long-distance mobility when overexpressed in *Nicotania benthiamana* (Toscano-Morales *et al.*, 2014). Movement across

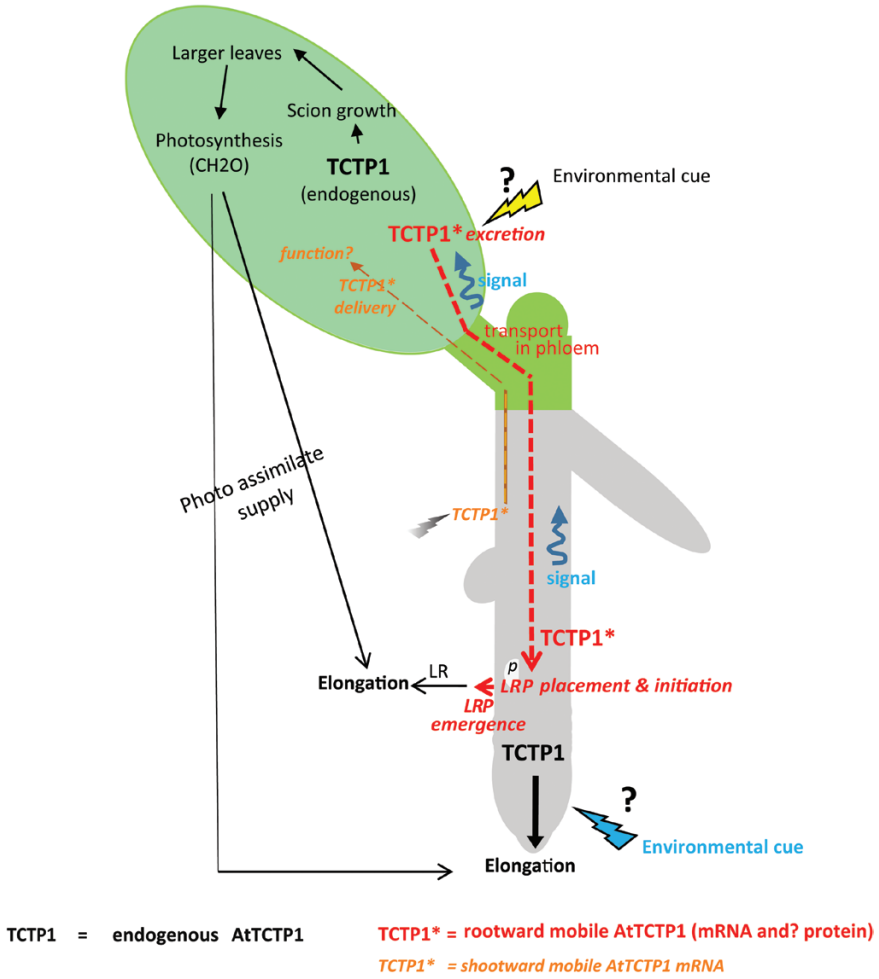

Fig. 6. Proposed model of synergistic regulation of root development by constitutive and mobile *AtTCTP1* gene products. Local constitutive *AtTCTP1* (black lettering and arrows) acts as a positive regulator of cell growth and proliferation within roots and aerial organs, and thus overall organ size. Overall root length is bounded by photoassimilate supply, and hence is indirectly dependent on AtTCTP1 constitutive expression in the shoot through its effects on the size of the photosynthetic apparatus. Mobile *AtTCTP1* mRNAs translocated from the shoot and encoded proteins (red lettering and arrows) act as systemic destination-selective signalling molecules to dynamically modulate the spatio-temporal patterning of lateral root initiation and emergence sites on the primary root, and the size of the LR formation zone, perhaps too the initial 'priming' step of pericycle LRP founder cells. The mechanisms flagging *AtTCTP1* gene product(s) for excretion and export to roots, and unloading in destination cells are unknown, but are probably regulated by a combination of above-ground and below-ground environmental cues in interaction with endogenous cues, including age-dependent cues. The dashed arrows depict 'movement'; solid arrows denote 'promotion'. *p* denotes the pericycle. Identified translocation of AtTCTP1 mRNAs from root to shoot—of unknown function—is also denoted (orange lettering and dashed arrows).

the graft junction appeared to correlate with the formation of aerial roots at the interface of the grafted stem segments (Toscano-Morales *et al.*, 2014). This raises the possibility of a broad role for *TCTP* mobile mRNAs/proteins in *de novo* root organogenesis, whether LRs or shoot-born roots, with specificity between gene isoforms in cell types targeted for developmental reprogramming and formation of root primordia from a variety of tissues (Bellini *et al.*, 2014), whichever is most appropriate.

Plant TCTP genes show high similarity among species. TCTP mRNAs and proteins have been detected in the vasculature of diverse species, including the monocot rice where the TCTP family is reduced to one member (Supplementary Table S1). This suggests that the mobility and extracellular signalling function of *AtTCTP1* to control root organogenesis might be widely conserved within the plant kingdom, and highly relevant to a better understanding of post-embryonic formation of lateral organs in plants, and the elusive coordination of shoot and root morphogenesis.

Supplementary data

Supplementary data are available at *JXB* online.

Fig. S1. TCTP1–GFP fluorescence is restricted to specific strands along the vasculature.

Fig. S2. Distinctive GFP fluorescence pattern in roots grafted to a *pTCTP1::gTCTP1-GFP* scion compared with a *p35S::GFP* scion.

Fig. S3. Time-course of appearance of TCTP1–GFP fluorescence in *pTCTP1::gTCTP1-GFP*/WT heterografts.

Fig. S4. Kinetics of scion expansion in homografts and heterografts between WT and TCTP-RNAi seedlings.

Fig. S5. Similar scion and primary root sizes in WT_{AMP} and TCTP1-RNAi scions following scion size normalization.

Fig. S6. Root patterning in TCTP1-RNAi seedlings shows no deviation from the stereotypical structure of WT Arabidopsis roots.

Fig. S7. At the same scion size, primary and overall lateral root lengths are independent of TCTP1 expression in the scion and mobility to the rootstock.

Fig. S8. The auxin transport inhibitor NPA does not modify GFP fluorescence of scion-derived TCTP1–GFP protein in the root.

Table S1. Plant TCTP/TCTP-like mRNAs or proteins detected as present in the vasculature or found to be moving through graft junctions, in published studies and publicly available databases.

Acknowledgements

This work was supported by The Australian National University and a Postgraduate Research Scholarship through the Australian Government Research Training Program.

References

Aoki K, Suzui N, Fujimaki S, Dohmae N, Yonekura-Sakakibara K, Fujiwara T, Hayashi H, Yamaya T, Sakakibara H. 2005. Destination-selective long-distance movement of phloem proteins. The Plant Cell **17**, 1801–1814.

Atkins CA, Smith PM, Rodriguez-Medina C. 2011. Macromolecules in phloem exudates—a review. Protoplasma **248**, 165–172.

Bai S, Kasai A, Yamada K, Li T, Harada T. 2011. A mobile signal transported over a long distance induces systemic transcriptional gene silencing in a grafted partner. Journal of Experimental Botany **62**, 4561–4570.

Banerjee AK, Lin T, Hannapel DJ. 2009. Untranslated regions of a mobile transcript mediate RNA metabolism. Plant Physiology **151**, 1831–1843.

Barreau C, Paillard L, Osborne HB. 2005. AU-rich elements and associated factors: are there unifying principles? Nucleic Acids Research **33**, 7138–7150.

Batailler B, Lemaître T, Vilaine F, Sanchez C, Renard D, Cayla T, Beneteau J, Dinant S. 2012. Soluble and filamentous proteins in Arabidopsis sieve elements. Plant, Cell & Environment **35**, 1258–1273.

Beeckman T, Burssens S, Inzé D. 2001. The peri-cell-cycle in Arabidopsis. Journal of Experimental Botany **52**, 403–411.

Bellini C, Pacurar DI, Perrone I. 2014. Adventitious roots and lateral roots: similarities and differences. Annual Review of Plant Biology **65**, 639–666.

Benitez-Alfonso Y, Faulkner C, Pendle A, Miyashima S, Helariutta Y, Maule A. 2013. Symplastic intercellular connectivity regulates lateral root patterning. Developmental Cell **26**, 136–147.

Berkowitz O, Jost R, Pollmann S, Masle J. 2008. Characterization of TCTP, the translationally controlled tumor protein, from *Arabidopsis thaliana*. The Plant Cell **20**, 3430–3447.

Betsch L, Boltz V, Brioudes F, Pontier G, 2019. TCTP and CSN4 control cell cycle progression and development by regulating CULLIN1 neddylation in plants and animals. PLoS Genetics **15**, e1007899.

Bommer U-A. 2017. The translational controlled tumour protein TCTP: biological functions and regulation. In: Telerman A, Amson R, eds. TCTP/tpt1—remodeling signaling from stem cell to disease. Cham: Springer International Publishing, 69–126.

Bommer UA, Thiele BJ. 2004. The translationally controlled tumour protein (TCTP). International Journal of Biochemistry & Cell Biology **36**, 379–385.

Brioudes F, Thierry A-M, Chambrier P, Mollereau B, Bendahmane M. 2010. Translationally controlled tumor protein is a conserved mitotic growth integrator in animals and plants. Proceedings of the National Academy of Sciences, USA **107**, 16384–9.

Calderwood A, Kopriva S, Morris RJ. 2016. Transcript abundance explains mRNA mobility data in *Arabidopsis thaliana*. The Plant Cell **28**, 610–615.

Cans C, Passer B. 2003. Translationally controlled tumor protein acts as a guanine nucleotide dissociation inhibitor on the translation elongation factor eEF1A. Proceedings of the National Academy of Sciences, USA **100**, 13892–13897.

Cao B, Lu Y, Chen G, Lei J. 2010. Functional characterization of the translationally controlled tumor protein (TCTP) gene associated with growth and defense response in cabbage. Plant Cell, Tissue and Organ Culture **103**, 217–226.

Casimiro I. 2001. Auxin transport promotes arabidopsis lateral root initiation. The Plant Cell **13**, 843–852.

Chen SH, Wu P-S, Chou C-H, Yan Y-T, Liu H, Weng S-Y, Yang-Yen H-F. 2007. A knockout mouse approach reveals that TCTP functions as an essential factor for cell proliferation and survival in a tissue- or cell type-specific manner. Molecular Biology of the Cell **18**, 2525–2532.

Chen Y, Chen X, Wang H, Bao Y, Zhang W. 2014. Examination of the leaf proteome during flooding stress and the induction of programmed cell death in maize. Proteome Science **12**, 1–18.

Corbesier L, Vincent C, Jang S, *et al.* 2007. FT protein movemen contributes to long-distance signaling in floral induction of Arabidopsis. Science **316**, 1030–1033.

de Carvalho M, Acencio ML, Laitz AVN, de Araújo LM, de Lara Campos Arcuri M, do Nascimento LC, Maia IG. 2017. Impacts of the overexpression of a tomato translationally controlled tumor protein (TCTP) in tobacco revealed by phenotypic and transcriptomic analysis. Plant Cell Reports **36**, 887–900.

Deng Z, Chen J, Leclercq J, Zhou Z, Liu C, Liu H, Yang H, Montoro P, Xia Z, Li D. 2016. Expression profiles, characterization and function of HbTCTP in rubber tree (*Hevea brasiliensis*). Frontiers in Plant Science **7**, 789.

De Rybel B, Vassileva V, Parizot B, *et al.* 2010. A novel aux/IAA28 signaling cascade activates GATA23-dependent specification of lateral root founder cell identity. Current Biology **20**, 1697–1706.

De Smet I, Lau S, Voss U, *et al.* 2010. Bimodular auxin response controls organogenesis in Arabidopsis. Proceedings of the National Academy of Sciences, USA **107**, 2705–2710.

De Smet I, Tetsumura T, De Rybel B, *et al.* 2007. Auxin-dependent regulation of lateral root positioning in the basal meristem of Arabidopsis. Development **134**, 681–690.

Dong X, Yang B, Li Y, Zhong C, Ding J. 2009. Molecular basis of the acceleration of the GDP–GTP exchange of human ras homolog enriched in brain by human translationally controlled tumor protein. Journal of Biological Chemistry **284**, 23754–23764.

Du B, Wei Z, Wang Z, Wang X, Peng X, Du B, Chen R, Zhu L, He G. 2015. Phloem-exudate proteome analysis of response to insect brown plant-hopper in rice. Journal of Plant Physiology **183**, 13–22.

Dubrovsky JG, Sauer M, Napsucialy-Mendivil S, Ivanchenko MG, Friml J, Shishkova S, Celenza J, Benkova E. 2008. Auxin acts as a local morphogenetic trigger to specify lateral root founder cells. Proceedings of the National Academy of Sciences, USA **105**, 8790–8794.

Freixes S, Thibaud M-C, Tardieu F, Muller B. 2002. Root elongation and branching is related to local hexose concentration in *Arabidopsis thaliana* seedlings. Plant, Cell & Environment **25**, 1357–1366.

French A, Ubeda-Tomás S, Holman TJ, Bennett MJ, Pridmore T. 2009. High-throughput quantification of root growth using a novel image-analysis tool. Plant Physiology **150**, 1784–1795.

Gawehns F, Ma L, Bruning O, Houterman PM, Boeren S, Cornelissen BJ, Rep M, Takken FL. 2015. The effector repertoire of *Fusarium oxysporum* determines the tomato xylem proteome composition following infection. Frontiers in Plant Science **6**, 967.

Haywood V, Yu TS, Huang NC, Lucas WJ. 2005. Phloem long-distance trafficking of GIBBERELLIC ACID-INSENSITIVE RNA regulates leaf development. The Plant Journal **42**, 49–68.

Hsu YC, Chern JJ, Cai Y, Liu M, Choi KW. 2007. Drosophila TCTP is essential for growth and proliferation through regulation of dRheb GTPase. Nature **445**, 785–788.

Jaeger KE, Wigge PA. 2007. FT protein acts as a long-range signal in Arabidopsis. Current Biology **17**, 1050–1054.

Jorgensen RA, Atkinson RG, Forster RL, Lucas WJ. 1998. An RNA-based information superhighway in plants. Science **279**, 1486–1487.

Kehr J, Kragler F. 2018. Long distance RNA movement. New Phytologist **218**, 29–40.

Kim G, LeBlanc ML, Wafula EK, dePamphilis CW, Westwood JH. 2014. Genomic-scale exchange of mRNA between a parasitic plant and its hosts. Science **345**, 808–811.

Kim M, Canio W, Kessler S, Sinha N. 2001. Developmental changes due to long-distance movement of a homeobox fusion transcript in tomato. Science **293**, 287–289.

Kim YM, Han YJ, Hwang OJ, Lee SS, Shin AY, Kim SY, Kim JI. 2012. Overexpression of Arabidopsis translationally controlled tumor protein gene AtTCTP enhances drought tolerance with rapid ABA-induced stomatal closure. Molecules and Cells **33**, 617–626.

Laskowski M, Grieneisen VA, Hofhuis H, Hove CA, Hogeweg P, Marée AF, Scheres B. 2008. Root system architecture from coupling cell shape to auxin transport. PLoS Biology **6**, e307.

Lee-Ho E, Walton LJ, Reid DM, Yeung EC, Kurepin LV. 2007. Effects of elevated carbon dioxide and sucrose concentrations on *Arabidopsis thaliana* root architecture and anatomy. Canadian Journal of Botany **85**, 324–330.

Lewis DR, Negi S, Sukumar P, Muday GK. 2011. Ethylene inhibits lateral root development, increases IAA transport and expression of PIN3 and PIN7 auxin efflux carriers. Development **138**, 3485–3495.

Li D, Deng Z, Liu X, Qin B. 2013. Molecular cloning, expression profiles and characterization of a novel translationally controlled tumor protein in rubber tree (*Hevea brasiliensis*). Journal of Plant Physiology **170**, 497–504.

Liang D, White RG, Waterhouse PM. 2012. Gene silencing in Arabidopsis spreads from the root to the shoot, through a gating barrier, by template-dependent, nonvascular, cell-to-cell movement. Plant Physiology **159**, 984–1000.

Livak KJ, Schmittgen TD. 2001. Analysis of relative gene expression data using real-time quantitative PCR and the 2(-Delta Delta C(T)) Method. Methods **25**, 402–408.

Lough TJ, Lucas WJ. 2006. Integrative plant biology: role of phloem long-distance macromolecular trafficking. Annual Review of Plant Biology **57**, 203–232.

Macdonald SM. 2012. Potential role of histamine releasing factor (HRF) as a therapeutic target for treating asthma and allergy. Journal of Asthma and Allergy **5**, 51–59.

MacDonald SM. 2017. History of histamine-releasing factor (HRF)/translationally controlled tumor protein (TCTP) including a potential therapeutic target in asthma and allergy. In: Telerman A, Amson R, eds. TCTP/tpt1—remodeling signaling from stem cell to disease. Cham: Springer International Publishing, 291–308.

MacDonald SM, Rafnar T, Langdon J, Lichtenstein LM. 1995. Molecular identification of an IgE-dependent histamine-releasing factor. Science **269**, 688–690.

Macgregor DR, Deak KI, Ingram PA, Malamy JE. 2008. Root system architecture in Arabidopsis grown in culture is regulated by sucrose uptake in the aerial tissues. The Plant Cell **20**, 2643–2660.

Malamy JE, Benfey PN. 1997. Organization and cell differentiation in lateral roots of *Arabidopsis thaliana*. Development **124**, 33–44.

Malter D, Wolf S. 2011. Melon phloem-sap proteome: developmental control and response to viral infection. Protoplasma **248**, 217–224.

Marsch-Martínez N, Franken J, Gonzalez-Aguilera KL, de Folter S, Angenent G, Alvarez-Buylla ER. 2013. An efficient flat-surface collar-free grafting method for *Arabidopsis thaliana* seedlings. Plant Methods **9**, 14.

Melnyk CW, Molnar A, Bassett A, Baulcombe DC. 2011. Mobile 24 nt small RNAs direct transcriptional gene silencing in the root meristems of *Arabidopsis thaliana*. Current Biology **21**, 1678–1683.

Melnyk CW, Schuster C, Leyser O, Meyerowitz EM. 2015. A developmental framework for graft formation and vascular reconnection in *Arabidopsis thaliana*. Current Biology **25**, 1306–1318.

Molnar A, Melnyk CW, Bassett A, Hardcastle TJ, Dunn R, Baulcombe DC. 2010. Small silencing RNAs in plants are mobile and direct epigenetic modification in recipient cells. Science **328**, 872–875.

Moreno-Risueno MA, Van Norman JM, Moreno A, Zhang J, Ahnert SE, Benfey PN. 2010. Oscillating gene expression determines competence for periodic Arabidopsis root branching. Science **329**, 1306–1311.

Morris RJ. 2018. On the selectivity, specificity and signalling potential of the long-distance movement of messenger RNA. Current Opinion in Plant Biology **43**, 1–7.

Mouchel CF, Briggs GC, Hardtke CS. 2004. Natural genetic variation in Arabidopsis identifies BREVIS RADIX, a novel regulator of cell proliferation and elongation in the root. Genes & Development **18**, 700–714.

Muraro D, Byrne H, King J, Bennett M. 2013. The role of auxin and cytokinin signalling in specifying the root architecture of *Arabidopsis thaliana*. Journal of Theoretical Biology **317**, 71–86.

Notaguchi M, Higashiyama T, Suzuki T. 2015. Identification of mRNAs that move over long distances using an RNA-Seq analysis of *Arabidopsis*/*Nicotiana benthamiana* heterografts. Plant & Cell Physiology **56**, 311–321.

Notaguchi M, Wolf S, Lucas WJ. 2012. Phloem-mobile Aux/IAA transcripts target to the root tip and modify root architecture. Journal of Integrative Plant Biology **54**, 760–772.

Paultre DSG, Gustin MP, Molnar A, Oparka KJ. 2016. Lost in transit: long-distance trafficking and phloem unloading of protein signals in Arabidopsis homografts. The Plant Cell **28**, 2016–2025.

Péret B, Larrieu A, Bennett MJ. 2009. Lateral root emergence: a difficult birth. Journal of Experimental Botany **60**, 3637–3643.

Péret B, Swarup K, Ferguson A, *et al.* 2012. AUX/LAX genes encode a family of auxin influx transporters that perform distinct functions during Arabidopsis development. The Plant Cell **24**, 2874–2885.

Ramakers C, Ruijter JM, Deprez RH, Moorman AF. 2003. Assumption-free analysis of quantitative real-time polymerase chain reaction (PCR) data. Neuroscience Letters **339**, 62–66.

Raya-González J, Pelagio-Flores R, López-Bucio J. 2012. The jasmonate receptor COI1 plays a role in jasmonate-induced lateral root formation and lateral root positioning in *Arabidopsis thaliana*. Journal of Plant Physiology **169**, 1348–1358.

Ross-Elliott TJ, Jensen KH, Haaning KS, *et al.* 2017. Phloem unloading in Arabidopsis roots is convective and regulated by the phloem-pole pericycle. eLife **6**, 1–31.

Stadler R, Wright KM, Lauterbach C, Amon G, Gahrtz M, Feuerstein A, Oparka KJ, Sauer N. 2005. Expression of GFP-fusions in Arabidopsis companion cells reveals non-specific protein trafficking into sieve elements and identifies a novel post-phloem domain in roots. The Plant Journal **41**, 319–331.

Thieme CJ, Rojas-Triana M, Stecyk E, *et al.* 2015. Endogenous Arabidopsis messenger RNAs transported to distant tissues. Nature Plants **1**, 15025.

Toscano-Morales R, Xoconostle-Cázares B, Martínez-Navarro AC, Ruiz-Medrano R. 2014. Long distance movement of an Arabidopsis Translationally Controlled Tumor Protein (AtTCTP2) mRNA and protein in tobacco. Frontiers in Plant Science **5**, 705.

Turgeon R, Wolf S. 2009. Phloem transport: cellular pathways and molecular trafficking. Annual Review of Plant Biology **60**, 207–221.

Turnbull CG, Lopez-Cobollo RM. 2013. Heavy traffic in the fast lane: long-distance signalling by macromolecules. New Phytologist **198**, 33–51.

Wu H, Gong W, Yao X, Wang J, Perrett S, Feng Y. 2015. Evolutionarily conserved binding of translationally controlled tumor protein to eukaryotic elongation factor 1B. Journal of Biological Chemistry **290**, 8694–8710.

Xia C, Zheng Y, Huang J, *et al.* 2018. Elucidation of the mechanisms of long-distance mRNA movement in a *Nicotiana benthamiana*/tomato heterograft system. Plant Physiology **177**, 745–758.

Yang Y, Mao L, Jittayasothorn Y, Kang Y, Jiao C, Fei Z, Zhong GY. 2015. Messenger RNA exchange between scions and rootstocks in grafted grapevines. BMC Plant Biology **15**, 251.

Zhang W, Thieme CJ, Kollwig G, Apelt F, Yang L, Winter N, Andresen N, Walther D, Kragler F. 2016. tRNA-related sequences trigger systemic mRNA transport in plants. The Plant Cell **28**, 1237–1249.

Zhang Z, Zheng Y, Ham BK, Chen J, Yoshida A, Kochian LV, Fei Z, Lucas WJ. 2016. Vascular-mediated signalling involved in early phosphate stress response in plants. Nature Plants **2**, 16033.